IDENTIFICATION OF GROUND TARGETS FROM SEQUENTIAL HRR RADAR SIGNATURES

Xuejun Liao, Paul Runkle, Yan Jiao, and Lawrence Carin
Department of Electrical and Computer Engineering
Duke University
Durham, NC 27708-0291

ABSTRACT

An approach to identifying ground targets from sequential high-range-resolution (HRR) radar signatures is presented. A hidden Markov model (HMM) is employed to model the sequential information contained in multi-aspect target signatures. Dominant range-amplitude features are extracted via RELAX for dimension reduction. A new distance measure is incorporated into the HMM to allow a direct matching operation in the feature domain without requiring interpolation. The approach is applied to the dataset of ten MSTAR targets and is shown to yield an average identification rate of 90.3% using sequential information from 6 degree angular spans.

1. INTRODUCTION

High range resolution (HRR) radar signatures are widely utilized for the challenging task of electromagnetic target identification. Two standard modes exist in implementing target identification using HRR signatures. One is to treat the HRR signatures at different viewing angles as independent observations, from which one makes a classification decision [1-4]. Another is to perform coherent processing on observations at multiple angles, to form a radar image, and proceed with identification in the image domain [5-6]. Since a given HRR signature collapses the target information into a one-dimensional function of time, significant discrimination information may be lost and ambiguities arise when an unknown target is being interrogated, especially when similar targets exist in the reference library. In contrast, the radar image gives resolution in both the range and cross-range dimensions, significantly aiding classification performance. However, to form a high-quality radar image, the data quality must be high to avoid phase errors [8] and range curvature. For the case of a moving ground target, the radar image will inevitably be blurred due to target and sensor motion.

The aforementioned radar image implicitly employs multiple HRR signatures, from multiple aperture positions. In this paper we take an alternative approach to processing the sequence of HRR waveforms, without the need to form an image. In particular, we utilize a hidden Markov model (HMM) to process features from the sequence of HRR waveforms, thereby exploiting underlying sequential information. In [9] we discuss the application of HMMs to modeling the statistical information in a sequential set of multi-aspect acoustic-scattering signatures, with this work extended here for multi-aspect processing of HRR data, for ground targets. For ground targets the target motion is confined to a plane, therefore the change of viewing angle primarily consists of aspect change, with the elevation kept approximately at a constant angle. Usually the ground targets have a rich set of scattering features, with these extracted here via RELAX processing. The algorithm is applied to the ten-target MSTAR data.

2. HMM PROCESSING OF SEQUENTIAL HRR DATA

Figure 1(a) represents a typical sensor-target configuration for airborne interrogation of a ground target. The airborne radar periodically transmits coherent pulses of microwave energy, which impinge the ground target at depression angle φ.

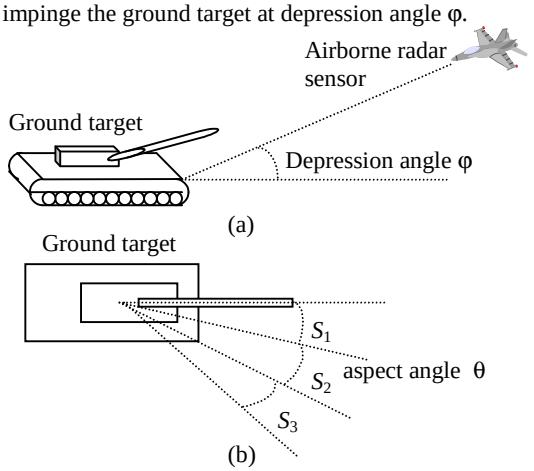

Fig. 1. State decomposition by dividing the full 360° aspect angle into a set of distinct angular sectors. (a) Three-dimensional geometry of the sensor-target configuration, (b) projection of the 3-D configuration onto the 2-D ground, assuming the depression angle remains approximately constant.

Each pulse is subsequently reflected from the target and received by the radar. After some pre-processing of these scattered radar echo pulses, a sequence of HRR signatures is obtained, each representative of the target as viewed from a distinct target-sensor orientation (with particular target-sensor orientations dependent on the sensor motion and target pose, with the latter typically unknown). The depression angle of the incident wave can be maintained as constant by controlling the

sensor flight path, with such assumed here. The variable target-sensor orientations are therefore modeled as a change in the azimuthal orientation (see Fig. 1b).

It is well known that HRR signatures exhibit significant variability as viewed from different orientations [1-4,7]. Nevertheless, there are typically contiguous angular sectors over which the scattered fields are approximately stationary statistically. Each such sector is termed a "state" (see Fig. 1b), and the sequence of HRR measurements sample waveforms from a sequence of target states, with this sequence well characterized via a Markov model [9]. In practice the target orientation is unknown (or "hidden"), in addition to the target identity, and therefore the sequence of scattered waveforms is modeled via a *hidden* Markov model (HMM).

Assume a target is partitioned into *N* distinct states, denoted $S=\{s_1,s_2,\cdots,s_N\}$. The HMM state transitions are denoted by the matrix $A=\{a_{ij}\}$, where a_{ij} is the probability of transiting from state *i* to state *j*. Further, the initial-state probabilities are denoted by the vector $\pi=\{\pi_i\}$ wherein i is the state index. For the sequence of HRR measurements, assume that $\delta\theta$ represents the maximum change in the target-sensor orientation, upon consecutive measurements (the change in orientation is assumed smaller than $\delta\theta$, which can be implemented by controlling the sensor flight path, while the absolute target-sensor orientation is assumed unknown). If θ_i represents the angular extent of state *i*, and assuming $\delta\theta<\theta_i$ for all *i*, then the matrix $A=\{a_{ij}\}$ is tri-diagonal, yielding the HMM construct in Fig. 2 (shown for four states).

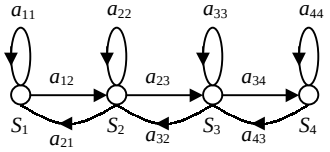

Fig 2. Illustration of state transition governed by a transition matrix with tri-diagonal structure

Based on the aforementioned assumptions with regard to $\delta\theta$ and θ_i, one can readily demonstrate the following estimations for $A=\{a_{ij}\}$

$$a_{i,i-1}=a_{i,i+1}=\delta\theta/(2\theta_i) \qquad a_{i,i}=(\theta_i-\delta\theta)/\theta_i \tag{1}$$

If the initial target pose is uniformly distributed, we similarly have

$$\pi_i=\theta_i\Big/\sum_{i=1}^{N}\theta_i \tag{2}$$

As discussed further below, (1) and (2) constitute initial estimates for $A=\{a_{ij}\}$ and $\pi=\{\pi_i\}$, with these refined via Baum-Welch training [14].

3. STATE-DEPENDENT STATISTICS

The model employed for the state-dependent statistics is dependent on the selected feature set. Ground targets usually contain fairly complex scattering features. Each of the HRR waveforms for the MSTAR data set consists of 72 range bins, and therefore use of the waveform itself, as a feature vector, is not an attractive option. Moreover, the HRR signature can be corrupted by noise, and weak scattering features may be highly contaminated, making direct use of the signature unreliable for classification. For our problem, the radar frequency is centered at 10 GHz with a bandwidth of 600 MHz, and therefore the target scattering is well represented as a series of diffractions from scattering centers on the target surface. We seek the extraction of these scattering-center features for representation of a feature vector.

Researchers have considered several models for electromagnetic scattering from targets. For example, Altes has devised a general target model [15], others have based their model on the geometric theory of diffraction (GTD) [5], employing damped-complex-exponential models [10-11,13], as well as a point-scatterer model [12]. We here perform feature parsing via the point-scatter model in [12], employing the RELAX algorithm described therein.

Consider the frequency-dependent, complex HRR waveform $\hat{\mathrm{x}}(\omega)$, scattered from a given target at a particular (generally unknown) target-sensor orientation. The RELAX algorithm [12] is used to extract point-scattered wavefronts from $\hat{\mathrm{x}}(\omega)$, from which the range (time) dependent HRR waveform is realized

$$\mathrm{x}(r)=\sum_{k=1}^{K}A_k^x w(r-r_k^x) \tag{3}$$

where $\mathrm{x}(r)$ is the Fourier transform of $\hat{\mathrm{x}}(\omega)$ after extracting these series of point scatterers, $A_k^x=\sigma_k^x exp(j\phi_k^x)$ is the complex amplitude of the *k*th wavefront (magnitude σ_k^x), $w(r)$ is the real window function used to represent the spatial support of the wavefronts (defined by system bandwidth), and *K* represents the number of RELAX-extracted wavefronts. In the work presented here $w(r)$ is a Gaussian with variance consistent with sensor bandwidth. For each complex HRR waveform (3) we define the real and positive function

$$\tilde{\mathrm{x}}(r)=\sum_{k=1}^{K}\sigma_k^x w(r-r_k^x) \tag{4}$$

Now consider two HRR signatures $\tilde{x}(r)$ and $\tilde{y}(r)$, for which we wish a distance measure. The distance is defined in terms of the correlation

$$\begin{aligned}C(x,y)&=\int \mathrm{dr}\tilde{x}(\mathrm{r})\tilde{y}(\mathrm{r})=\sum_{k=1}^{K}\sum_{i=1}^{K}\sigma_k^x\sigma_i^y\int \mathrm{w}(\mathrm{r}-\mathrm{r}_k^x)\mathrm{w}(\mathrm{r}-\mathrm{r}_i^y)\mathrm{dr}\\&=\sum_{k=1}^{K}\sum_{i=1}^{K}\sigma_k^x\sigma_i^y\mathrm{g}(\mathrm{r}_k^x-\mathrm{r}_i^y)\end{aligned} \tag{5}$$

Since $w(r)$ is Gaussian, so is $g(r)$, with twice the variance. Using matrix notation, (5) can be re-written as

$$C(x,y)=\hat{\mathbf{o}}_x^T\mathbf{W}_{xy}\hat{\mathbf{o}}_y \tag{6}$$

with $\mathbf{W}_{xy}$ a $K\times K$ matrix representing the functions $g(r_k^x-r_i^y)$. Note that the correlation in (5) can be computed directly from the RELAX outputs, without having to explicitly form the range profile (4).

We now define the distance

$$d^2(x,y)=\hat{\mathbf{o}}_x^T\mathbf{W}_{xx}\hat{\mathbf{o}}_x+\hat{\mathbf{o}}_y^T\mathbf{W}_{yy}\hat{\mathbf{o}}_y-2\hat{\mathbf{o}}_x^T\mathbf{W}_{xy}\hat{\mathbf{o}}_y \tag{7}$$

which is referred to as the spatially weighted distance (SWD), in which each element in the weighting matrix is a function of

spatial distance between scatterers. In (7) $\mathbf{W}_{xx}$ and $\mathbf{W}_{yy}$ are of the same form as $\mathbf{W}_{xy}$. Note that if the wavefronts are spaced uniformly, such that $\Delta = r_{k+1}^x - r_k^x = r_{i+1}^y - r_i^y$ and $g(\Delta) = 0$, then this distance measure reduces to the traditional Euclidean distance

$$d^2(x,y) = \mathbf{ó}_x^T \mathbf{ó}_x + \mathbf{ó}_y^T \mathbf{ó}_y - 2\mathbf{ó}_x^T \mathbf{ó}_y = (\mathbf{ó}_x - \mathbf{ó}_y)^T (\mathbf{ó}_x - \mathbf{ó}_y) \quad (8)$$

The distance measure in (7) plays a pivotal role in the HRR HMM, as currently designed. In particular, for the N states $S=\{s_1, s_2, \cdots, s_N\}$ characteristic of a given target, we define a codebook of N codes $C = \{c_1, c_2, \cdots, c_N\}$, with code c_n associated with state s_n. Recall that the HMM requires a state-dependent statistical measure. For a given HRR signal x the likelihood that x is associated with state s_n is defined as

$$p(\mathrm{x}|s_n) = \frac{1}{\sqrt{2\pi\eta}} \exp[-\frac{d^2(\mathrm{x}, c_n)}{2\eta^2}] \quad (9)$$

The likelihood in (9) is clearly motivated by a Gaussian distribution, but here we explicitly utilize the distance measure d^2, which is tied to the RELAX features extracted from the HRR waveform.

Note that each target will have its own set of states and codes, and an important issue concerns the design of the state-dependent codes $C = \{c_1, c_2, \cdots, c_N\}$. As we discuss in the Conclusion, the sophisticated design of C is an area of future research. In the work reported here we simply utilize the training data associated with a given state to define the average HRR profile, this defining the code associated with that state. In (9) η^2 is the ensemble average of the SWD between the state-dependent HRR profiles and the associated code (averaged across all target states). The optimal state decomposition is also an area of future research, for in the work reported here we simply utilize a uniform state decomposition. We note, however, that the state-transition matrix, initial-state probabilities and the constant η^2 are optimized during Baum-Welch [14] optimization, based on training data. However, the target-dependent codebook C currently remains fixed. As discussed in Sec. 4, the training and testing data are distinct.

Summarizing the algorithm, each target is segmented into a uniformly distributed set of states, each state ideally representative of a set of target-sensor orientations over which the scattered fields are stationary. For each state we define an associated code, composed of representative RELAX features. In the testing phase we measure a sequence of HRR waveforms, and compute an overall HMM likelihood that the sequence is associated with a particular target. In the HMM we require the likelihood that a particular set of RELAX features, associated with a particular HRR waveform, is consistent with a given HMM state. This likelihood is computed using the distance between the RELAX features and the state-dependent code, with the distance computed as in (7), and the likelihood as in (9). The training data is used to define the target-dependent codes and optimize the HMM state-transition matrix and initial-state probability vector.

4. IDENTIFICATION RESULTS

We present example identification results using the approach discussed above. The data set used consists of the X-band HRR signatures of ten MSTAR targets (see [5,6] for details on the MSTAR targets). The MSTAR data set typically consists of image chips. These images have been converted into a sequence of HRR waveforms, through various filtering operations. The HRR data was provided to the investigators by the US Defense Advanced Research Projects Agency (DARPA), with the conversion of MSTAR images to HRR waveforms performed under the TRUMPETS program. All ground-based targets are of very similar shape (most are military vehicles, although there are a few civilian vehicles [5,6]).

The HRR signatures have a bandwidth of approximately 600MHz cantered at 10 GHz, and have a range resolution of approximately 0.3 meters. Training data and testing data are distinct (as provided by DARPA), each having a full coverage of 360° aspect angles (fixed depression angle). Recall that the HMM processes a sequence of HRR waveforms, without explicitly forming an image. The angular sampling is $\delta\theta = 0.1^o$ and the sequences are assumed to consist of sixty HRR waveforms (consistent with a 6^o aperture). For each target 3,601 signatures are used to cover the full 360° aspect range, resulting in a total of 36,010 training signatures and 36,010 testing signatures for the ten targets. The HRR signatures (complex) are transformed to the frequency domain and the RELAX algorithm [12] is employed to extract the features from the frequency domain data. To facilitate data manipulation, a fixed number of dominant point scatterers are extracted for each signature. Here we set this number as K=15 (see (3)). Each target is partitioned into 180 uniformly distributed states, each with $\theta_i = 2^o$ (see (1) and (2)). Ten HMM models are obtained, each describing one of the ten targets, and a maximum-likelihood (ML) classification is employed.

To evaluate classification performance, we use all possible sequences of sixty HRR waveforms (equivalently, all possible 6° apertures), yielding a total of 3,541 testing sequences for each target. Based on the frequency with which the testing sequences are assigned to each target, we obtain the confusion matrix shown in Table 1. The *ij*-th entry in the confusion matrix gives the percentage of target *i* identified as target *j* given that target *i* is the true target. It is seen that using our HMM-based approach, an average correct identification rate of 90.3% is attained for the ten MSTAR targets (the data considered is as given by DARPA, no additive noise is considered in these results).

To compare our approach with traditional techniques, we use the same training data to examine a Majority Voting Classifier (MVC) and an Independent Multi-aspect Classifier (IMC). For each target we have 180 states, along with associated codes and likelihoods (see (9)). In the MVC, each of the sixty HRR waveforms in the testing sequence is mapped to one of the target states, in a ML sense, using (9). Assume M_i represents the number of times a state from target *i* was so mapped into. The data under test is declared scattered from target *i* if $M_i > M_k$ for all targets *k* (ties are settled via an appropriately weighted random-number generator, *e.g.* 50/50 for a two-way tie). Note that the MVC does not exploit the fact that in reality all sixty waveforms come from the same target. The IMC utilizes this in a simple way. In particular, when testing if the HRR sequence is associated with target *i*, each HRR signature is associated with the state of target *i* for which (9) is largest, and the likelihood is computed as the product of the sixty associated likelihoods

(independence assumed). Both classifiers utilize pieces of the HMM, but do not utilize correlated sequential information, with this accounted for by the HMM.

The same HRR data considered by the HMM is also used to test the performance of the MVC and IMC. Space limitations preclude presentation of the complete confusion matrix for these simpler methods, but the average performance of the MVC and IMC algorithms was 62% and 58%, respectively. The degraded performance of the two classifiers is not surprising. The ten MSTAR targets are very confusing targets [5,6]. The HRR signature of a target at one aspect angle will quite likely be similar to the signature of another target at the same or some other aspect angle. This confusion will inevitably result in many wrong decisions for each individual signature. In contrast, similar signatures from two different targets will be much less likely to appear in the same order of aspect angles. That is, the sequential characteristics of signatures can be distinguishable even if the signatures themselves are confusing. It is the efficient use of this sequential information that gives the superior performance of the HMM model.

5. CONCLUSIONS

In this paper we have discussed the use of sequential information in identification of ground targets using HRR radar signatures. The underlying association of states to aspect angular sectors yields a simple and reliable setting for computation of the HMM parameters. The complexity of scattering from ground targets is made manageable by extracting parameters (features) of dominant scatterers. The Euclidean distance is extended to account for the general wavefront time of arrival, which then provides a statistical model for the HRR signals in a HMM state. It is shown that an average correct identification rate of 90.3% is achieved on the MSTAR data using information from 6° angular spans. While the results reported here are encouraging, there is much room for improvement. In particular, we are currently employing genetic algorithms to optimize the target state decomposition and definition of the target- and state-dependent codes.

REFERENCES

[1] H. J. Li and S. H. Yang, "Using range profiles as feature vectors to identify aerospace objects", *IEEE Trans. Antennas and Propagation*, Vol.41, No.3, pp.261-268, 1993.

[2] S. Hudson and D. Psaltis, "Correlation filters for aircraft identification from radar range profiles", *IEEE Trans. Aero. and Electronics System*, Vol. 29, No.3, pp. 741-748, 1993.

[3] A. Zyweck and R. E. Bogner, "Radar target classification of commercial aircraft", *IEEE Trans. Aerospace and Electronics System*, Vol.32, No.2, pp.598-606, 1996.

[4] R.A. Mitchell and J.J. Westerkamp, "Robust statistical feature based aircraft identification", *IEEE Trans. Aerospace and Electronic Systems*, Vol. 35, No.3, pp.1077-1094, 1999.

[5] H.-C. Chiang, R. L. Moses, and L.C. Potter, "Model-based classification of radar images", *IEEE Trans. Information Theory*, Vol.46, No.5, pp. 1842-1854, 2000.

[6] L.M Novak, "State-of-the-art of SAR automatic target recognition", The Record of the IEEE 2000 International Radar Conference, 2000, pp. 836 –843, 2000.

[7] X. Liao, Z. Bao, and M. Xing, "On the aspect sensitivity of high resolution range profiles and its reduction methods", The Record of the IEEE 2000 International Radar Conference, 2000, pp. 310–315, 2000.

[8] C.V. Jakowatz *et al*., *Spotlight-Mode Synthetic Aperture Radar: A Signal Processing Approach*, Kluwer Academic Press.

[9] P.R. Runckle, *et al*., "Hidden Markov models for multiaspect classification", *IEEE Trans. Signal Processing*, Vol. 47, No.7, pp.2035-2040, 1999.

[10]M.R. McClure, R.C. Qiu, and L. Carin, "On superresolution identification of observables from swept-frequency scattering data", *IEEE Trans. Anternnsa and Propagation*, Vol. 45, No.4, pp.631-641, 1997.

[11] T.K. Sarkar and O. Pereira, "Using the matrix pencil method to estimate the parameters of a sum of complex exponentials", *IEEE Antennas and Propagation Magazine"*, Vol. 37, No.1, pp.48-55, 1995.

[12] J. Li, P. Stoica, "Efficient mixed-spectrum estimation with application to target feature extraction", *IEEE Trans. Signal Processing*, Vol.44, No.2, pp.281-295, 1996.

[13] R. Carriere and R.L. Moses, "High resolution radar target modeling using modified Prony estimator", *IEEE Trans. Antennas and Propagation*, Vol.40, No.1, pp.13-18, 1992.

[14] L.R. Rabiner, "A tutorial on hidden Markov models and selected applications in speech recognition", P*roc. IEEE*, Vol. 77, No. 2, pp. 257 –286, 1989 .

[15] R. A. Altes, "Sonar for general target description and its similarity to animal echolocation systems", *J. of Acoust. Soc. Am.*, Vol. 59, No. 1, Jan. 1976.

	T72	BTR70	BMP2	2S1	ZSU234	BTR60	BRDM2	D7	T62	ZIL131
T72	92.1	0.31	0.68	1.52	0.82	0.37	1.44	1.07	0.40	1.30
BTR70	1.02	87.0	4.29	1.81	0.14	2.01	3.02	0	0.71	0
BMP2	0.14	0.96	89.2	4.77	2.20	0.37	1.52	0	0	0.79
2S1	0	2.51	1.64	85.4	0.08	1.33	4.80	0	1.30	2.94
ZSU234	0	0.88	1.38	0.40	89.0	1.19	0.51	3.22	1.95	1.47
BTR60	0	0.79	0.23	0.08	2.06	92.6	1.75	0.85	0.11	1.50
BRDM2	0.11	4.12	1.04	2.85	0	0.17	91.5	0.17	0	0
D7	0.96	0	0.11	0.08	0	0	0.51	98.0	0.31	0
T62	0	0.17	0.59	0.28	2.51	1.16	0.20	5.85	88.3	0.96
ZIL131	1.02	0.31	3.67	1.02	1.75	0	0	2.51	0.03	89.7

Table 1. Confusion matrix of the HMM classifier. The *ij*-th entry is percentage (%) of target *i* identified as target *j* given that target *i* is the true target (average rate: 90.29%).